

Figure S1

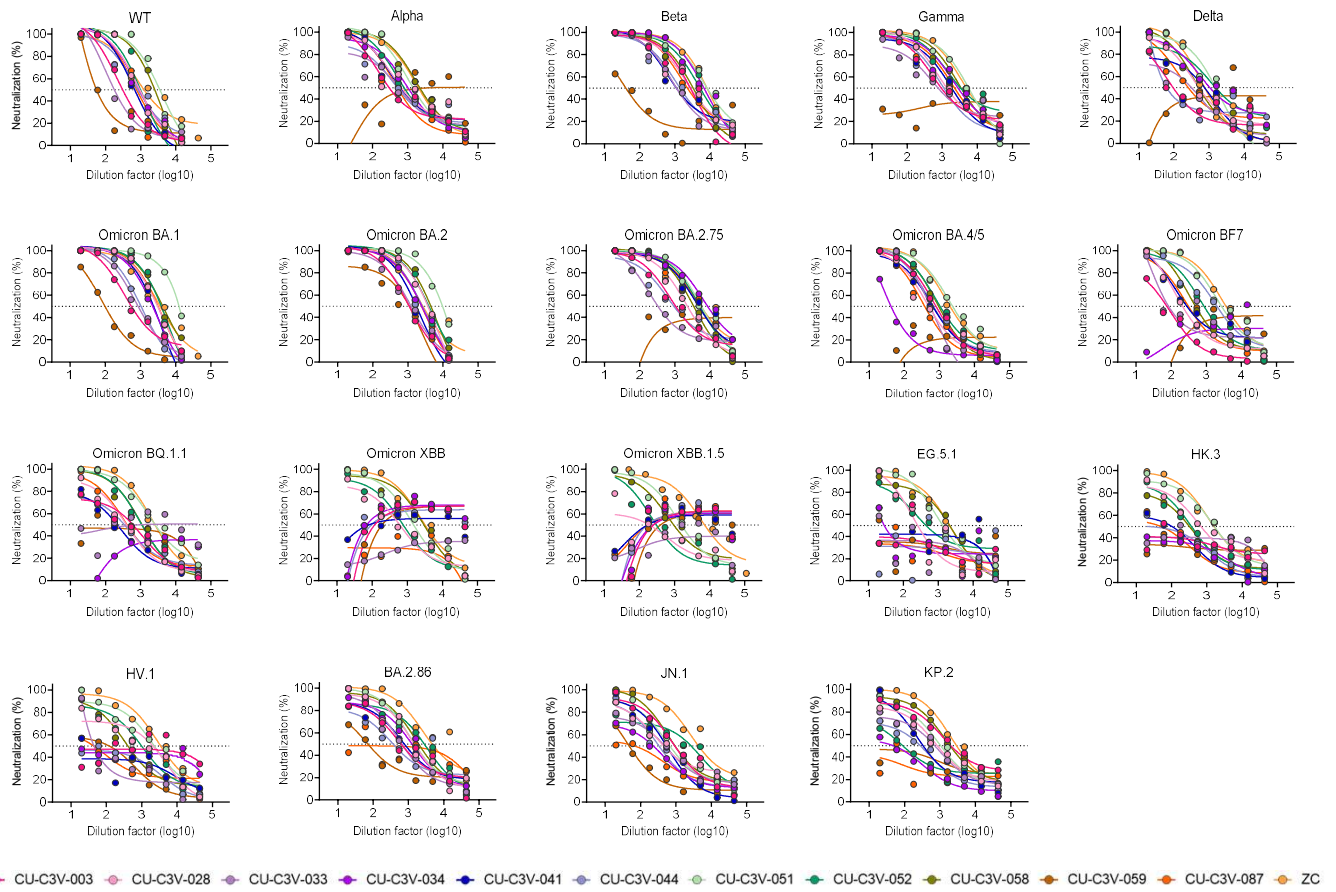
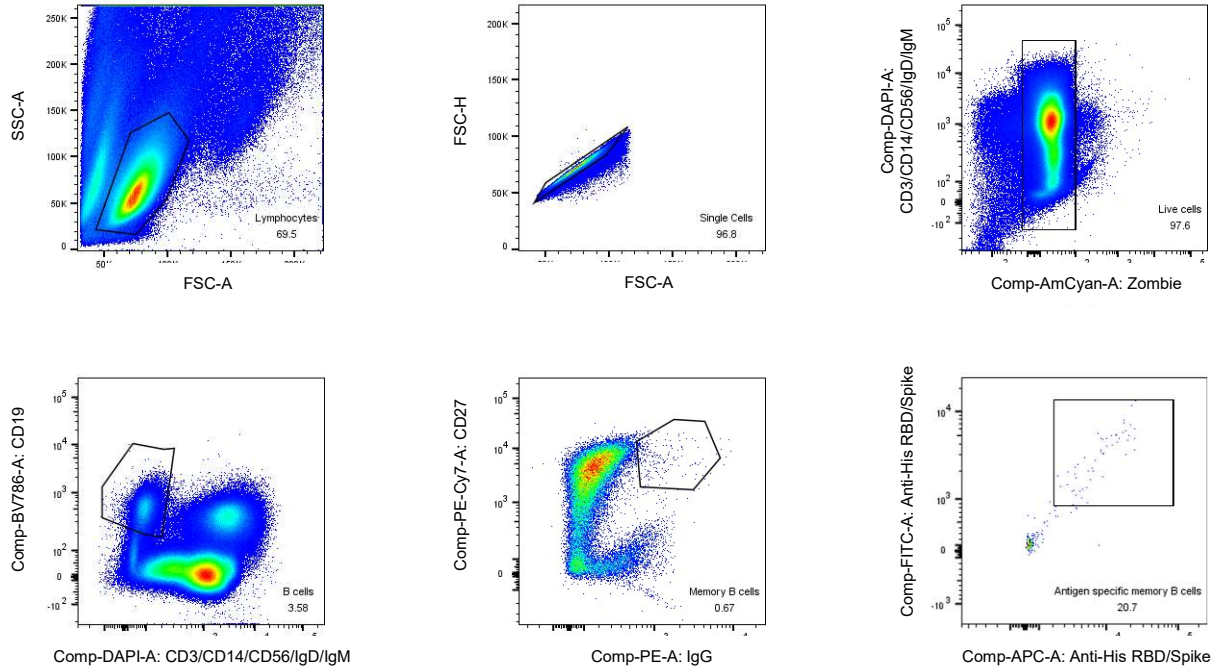


Figure S1. Neutralization of sera antibodies from a cohort of 12 Omicron breakthrough infection convalescents against pseudotyped WT and 18 variants.

The dashed line in each graph indicates 50% neutralization. CU, BA.2 breakthrough infection convalescents; ZC, BA.5 breakthrough infection convalescents.

A

3-dose SinoV/BNT vaccination+BA.2 breakthrough infection



B

3-dose BNT vaccination+BA.5 breakthrough infection

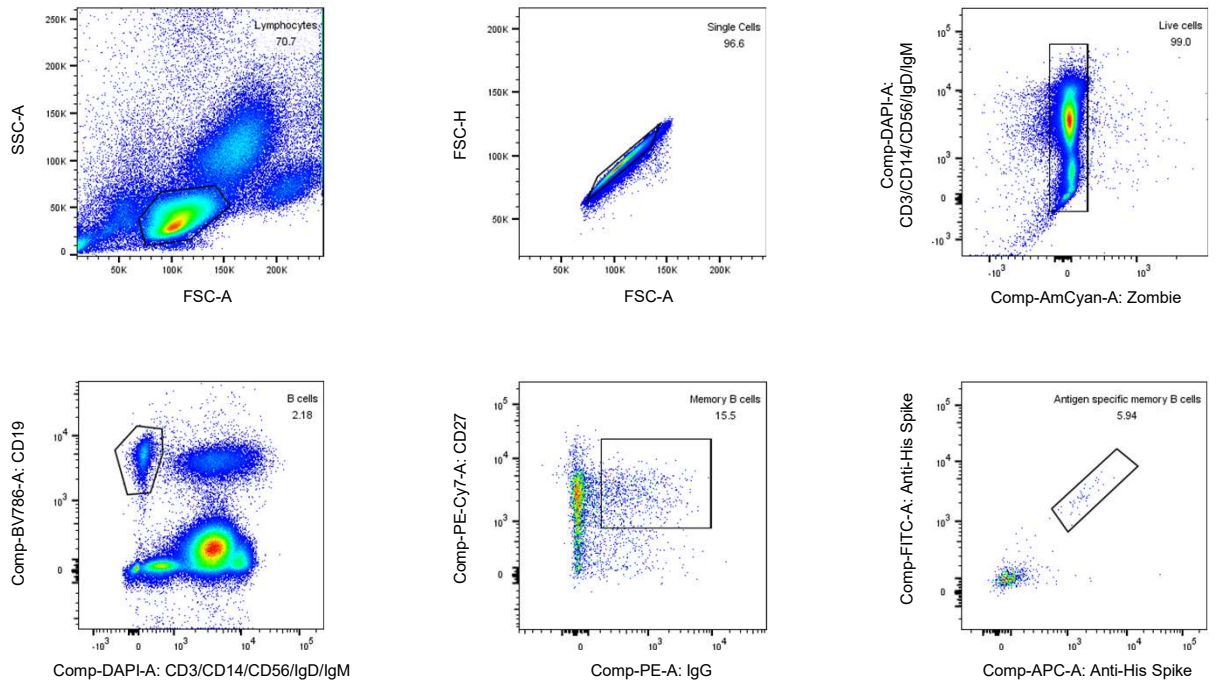


Figure S2. FACS (Fluorescence-activated cell sorting) analysis of antigen-specific immunoglobulin G-positive (IgG+) memory B cells from Omicron breakthrough infection convalescents.

A-B. FACS sorting of PBMCs from CUs (Sinovac, n = 5; BNT162b2, n = 6) (A) and ZC (BNT162b2, n = 1) (B) are shown. PBMCs were sorted into a SARS-CoV-2 RBD/spike-specific CD19⁺CD27⁺IgG⁺ subset.

Figure S4

		EC ₅₀ (ng/mL)		Competition ELISA			
		Class	Antibody	S2E12	LY-CoV555	LY-CoV1404	S2X259
RBD	G1	III	CUP2G3	72	91	22	30
		III	ZCP1B3	54	57	30	29
		--	ZCP1C3	29	25	29	-23
		III/III	ZCP2D4	55	46	40	-42
		III	ZCP2G5-2	79	67	-13	-47
		I	ZCP2G6-1	35	26	-8	-55
		II	ZCP3B4	25	48	16	4
		II	ZCP4C9	20	38	-17	17
		III	ZCP4D5-1	48	72	-5	11
	G2	I	ZCP1B5-2	36	25	-38	23
		III	ZCP1B7-1	76	72	33	-7
		--	ZCP1F7	17	13	-3	-4
		III/III	ZCP2B10	30	71	67	-34
		I	ZCP2C11-2	42	24	26	-39
		III	ZCP2G11	44	90	-6	6
	G3	III	CUP3C9	27	32	49	-22
		--	ZCP2C2	11	-13	-17	-18
		--	ZCP2D5	21	-22	-11	-24
		III	ZCP4C2	3	-9	44	-15

Competition (%)

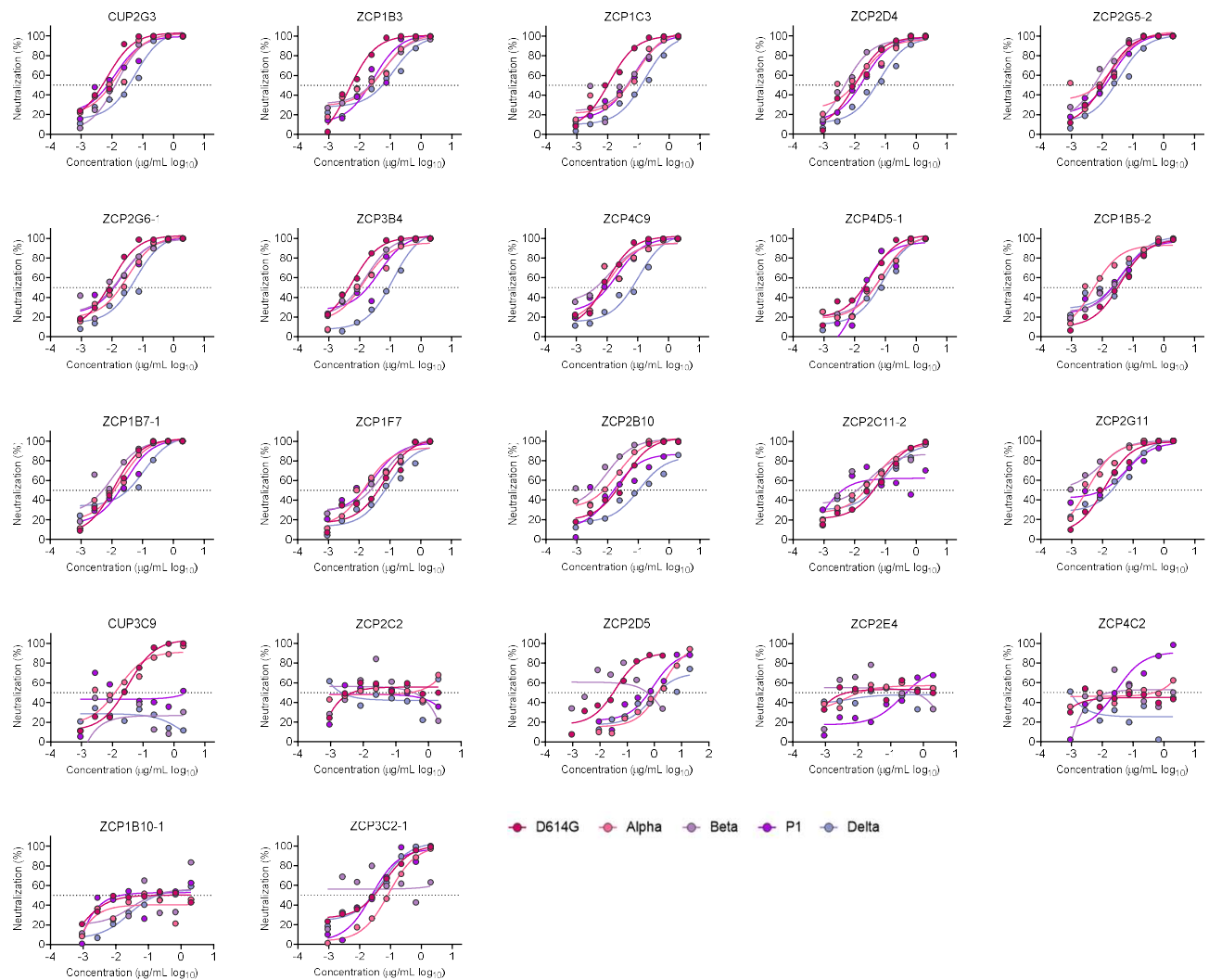
	>80
	35-80
	<35

Figure S4. Epitope mapping of 20 newly identified RBD-specific NAbs as determined by the competition ELISA.

The competition results of NAbs in blocking binding of biotinylated antibody targets (S2E12, LY-CoV555, LY-CoV1404 and S2X259) to the WT (D614G) spike trimer are shown by the ratio of area under curve (AUC) difference between targets in the presence of competitors and of competitor-free control, expressed as a percentage. No competitive binding (<35%), partially competitive binding (35-80%) and totally competitive binding (>80%) are indicated with gradient color. The top three ultrapotent bnAbs are highlighted in red.

Figure S5

A



B

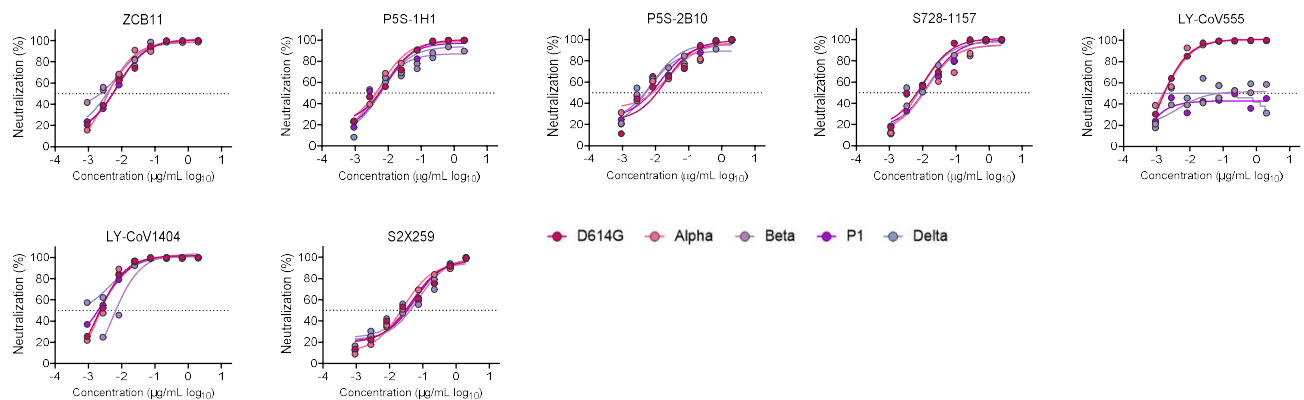
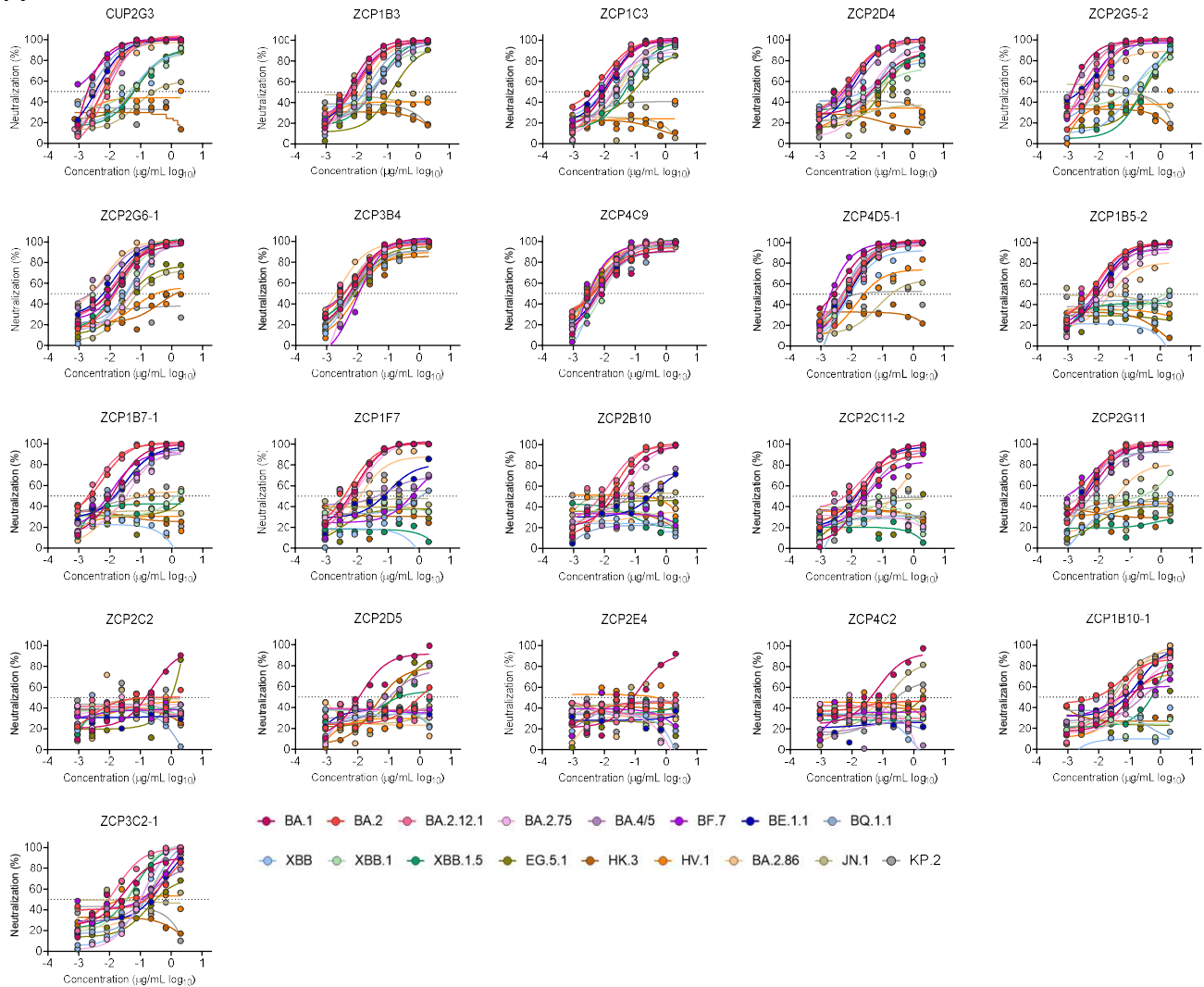


Figure S5. Quantitative neutralization measurement of 22 newly identified NAbs.

A-B. Neutralizing activity of 22 NAbs (A) and 7 published antibodies from class I-IV (B) against pseudotyped SARS-CoV-2 WT (D614G), Alpha, Beta, Gamma and Delta. The dashed line in each graph indicates 50% neutralization.

Figure S6

A



B

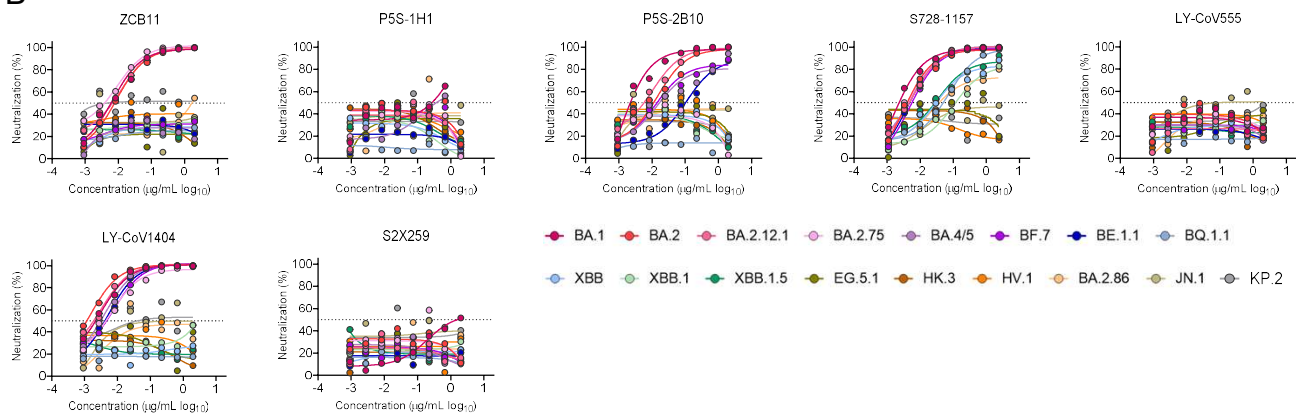
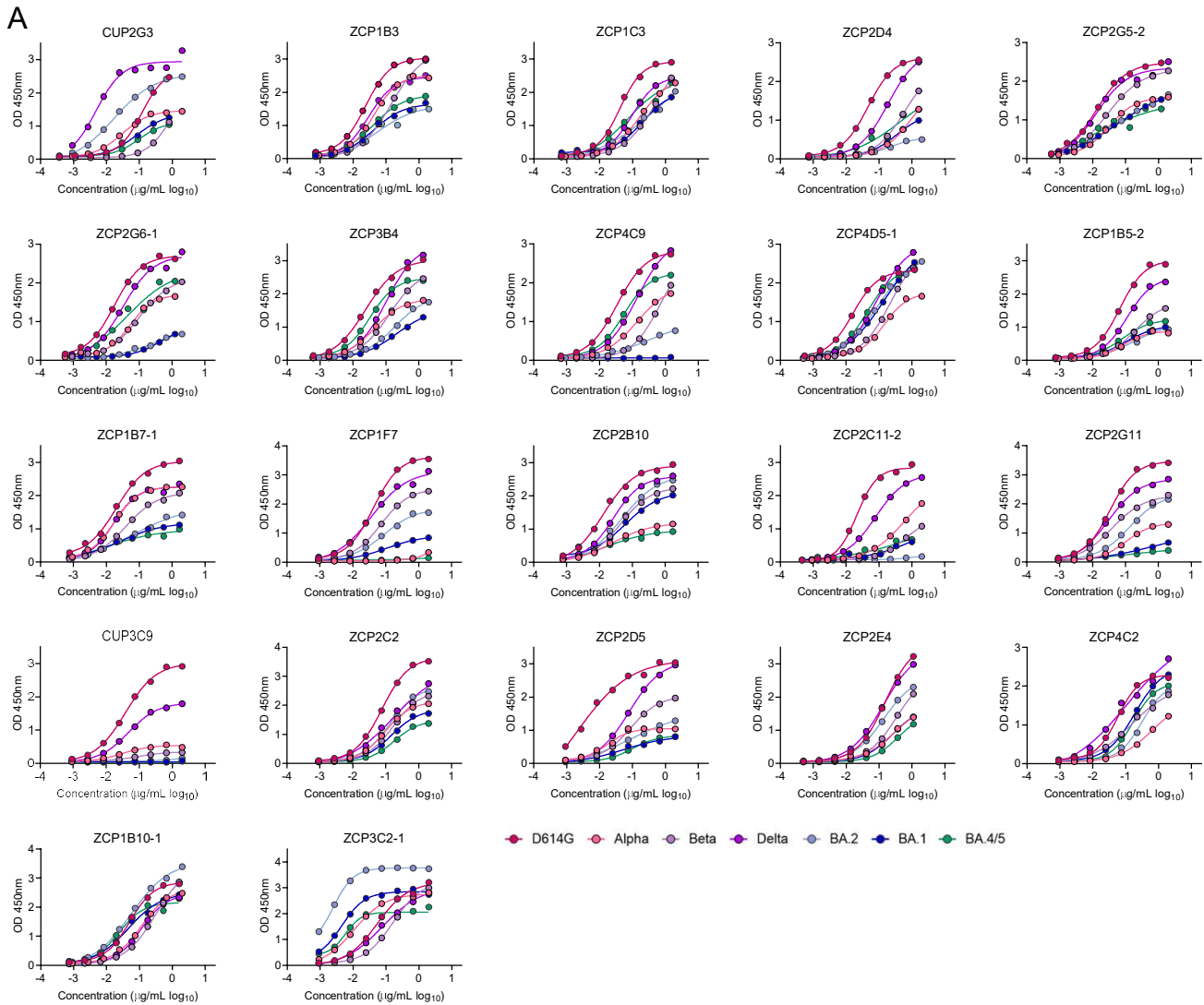


Figure S6. Quantitative neutralization measurement of 21 newly identified NAbs.

A-B. Neutralizing activity of 21 NABs (A) and published antibodies from class I-IV (B) against pseudotyped Omicron BA.1, BA.2, BA.4/5 and other subvariants. The dashed line in each graph indicates 50% neutralization.

Figure S7



B

	Class	Antibody	EC ₅₀ (ng/mL)		Binding activity to spike trimers						
			WT+	D614G	Alpha	Beta	Delta	BA.1	BA.2	BA.4/5	
RBD	G1	I CUP2G3	118.2	29.6	907.9	4.8	81.5	16.3	96.5		
		III ZCP1B3	24.0	42.7	144.9	29.7	40.5	54.4	39.8		
		-- ZCP1C3	41.5	168.4	577.9	93.0	200.2	772.6	71.5		
		III/III ZCP2D4	46.2	1091.0	571.8	186.2	343.7	--	433.7		
		III ZCP2G5-2	13.0	31.1	27.9	12.4	55.9	51.7	3.9		
		I ZCP2G6-1	17.5	53.9	99.6	31.9	413.1	249.9	42.7		
		I ZCP3B4	23.9	43.9	128.9	103.6	213.5	190.5	33.1		
		I ZCP4C9	34.5	137.6	682.7	136.7	--	320.0	53.8		
		I ZCP4D5-1	16.0	140.6	215.7	86.4	138.1	87.4	43.5		
RBD	G2	I ZCP1B5-2	67.1	88.8	197.2	112.1	101.3	184.1	80.8		
		III ZCP1B7-1	19.9	16.9	38.8	16.8	26.6	63.0	6.6		
		-- ZCP1F7	42.6	--	71.0	36.5	106.1	90.2	--		
		III/III ZCP2B10	12.9	25.0	43.3	26.2	61.4	48.5	16.1		
		I ZCP2C11-2	21.5	576.1	662.6	78.2	993.6	--	1189.0		
		III ZCP2G11	33.8	103.3	39.5	30.4	755.9	135.5	--		
		RBD	G3	III CUP3C9	38.3	--	--	47.7	--	--	--
-- ZCP2C2	76.2			95.9	170.8	169.3	147.9	135.2	181.3		
-- ZCP2D5	2.0			17.5	86.9	79.9	52.1	94.1	99.6		
-- ZCP2E4	154.2			302.5	345.2	132.7	262.8	136.5	384.2		
III ZCP4C2	57.5			629.3	148.8	107.6	187.9	311.6	169.9		
NTD	G4	-- ZCP1B10-1	49.7	115.0	316.2	114.0	46.2	54.8	23.7		
		-- ZCP3C2-1	53.9	10.5	165.0	76.7	4.5	2.5	5.9		

EC₅₀ (ng/mL) color scale: ≤10 (red), 50 (orange), 100 (yellow), 1000 (green), >1000 (light green).

Figure S7. Binding profile of 22 newly identified NAbs to various spike trimers.

(A) Binding activity of NAbs to WT (D614G) and VOC spike trimers as determined by ELISA at serial dilutions.

(B) Summary of EC₅₀ values. The level of activity is indicated according to the color bar. The top three ultrapotent bnAbs are highlighted in red.

Figure S8

A

		VL			
Identity (%)		ZCP1B7-1	ZCP2G5-2	ZCP2G11	CUP2G3
VH	ZCP1B7-1	--	99.2	99.2	99.2
	ZCP2G5-2	99.1	--	100	100
	ZCP2G11	99.1	98.2	--	100
	CUP2G3	99.1	100	98.2	--

B

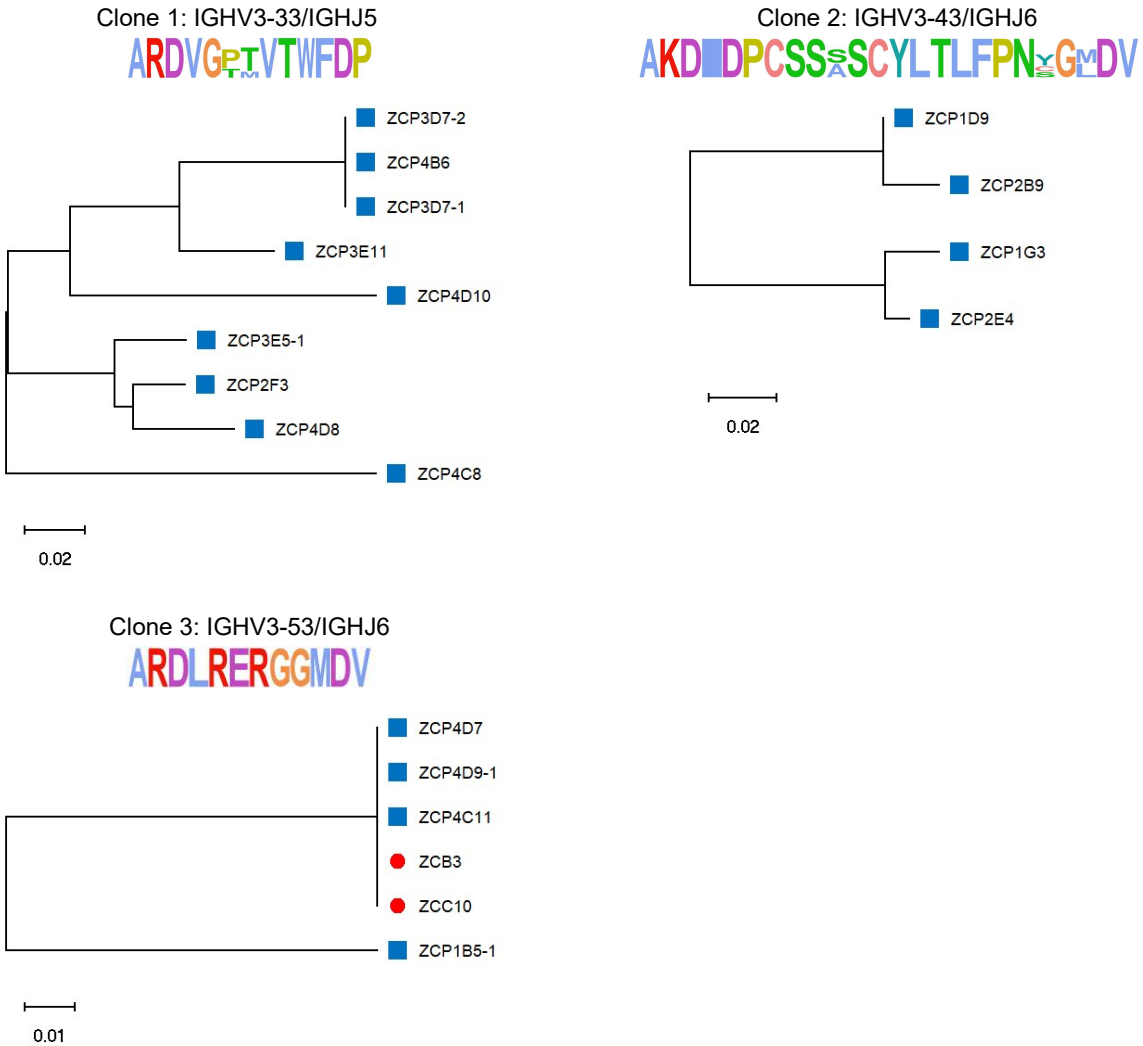


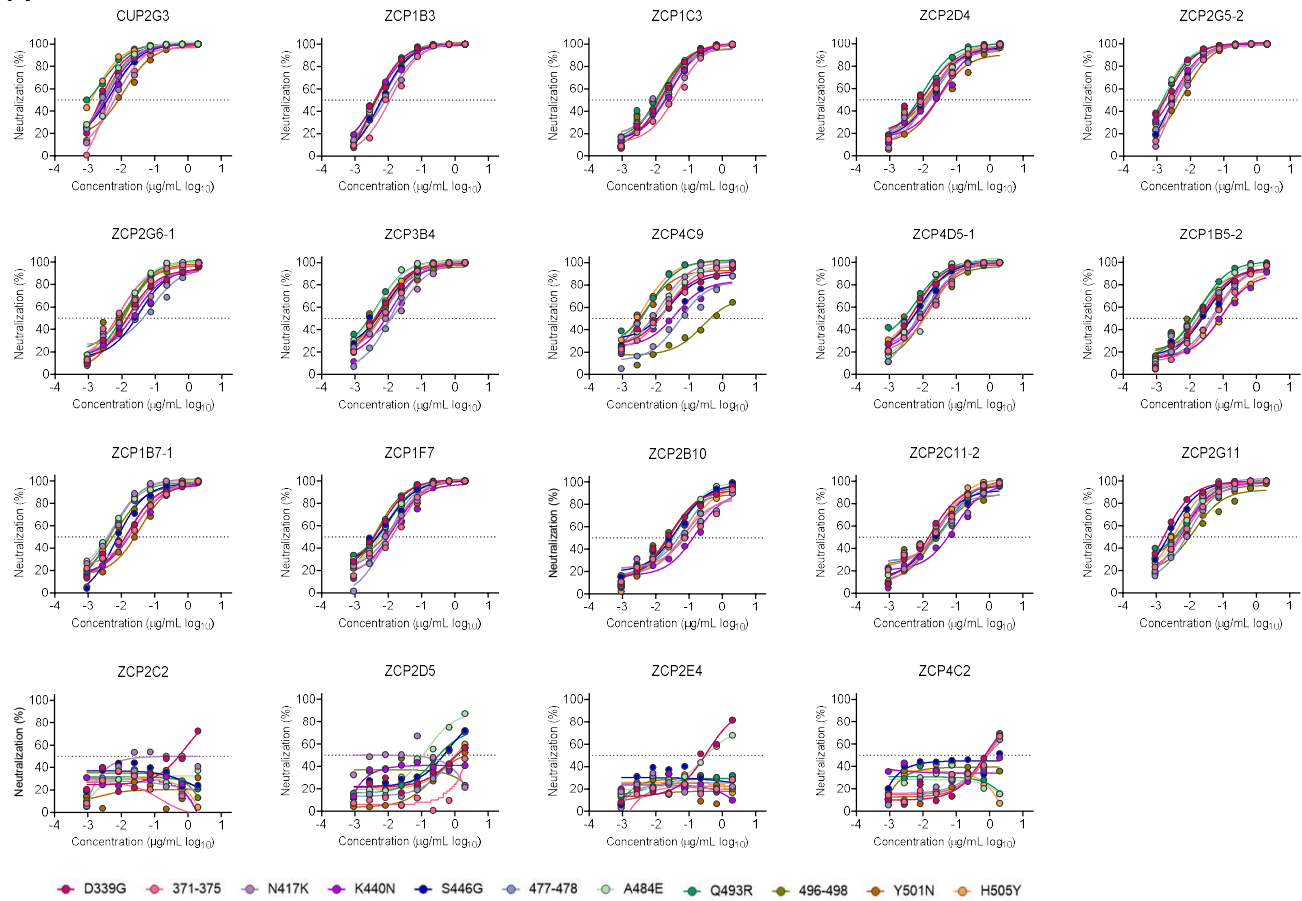
Figure S8. Sequence similarity and clonal relatedness among recovered mAbs.

(A) Pairwise comparison of V_H and V_L amino acid sequences of four identified IGHV4-39/IGKV1-NL1 NAbs.

(B) Phylogenetic trees for three clones identified from recovered ZC mAbs. Red dots and blue squares represent pre-existing mAbs elicited by WT-based vaccine and newly identified mAbs induced by BA.5 breakthrough infection, respectively.

Figure S9

A



B

		IC ₅₀ (ng/mL)	BA.1 reversed mutations									
Class	Antibody	D339G	371-375	N417K	K440N	S446G	477-478	A484E	R493Q	496-498	Y501N	H505Y
G1	I CUP2G3	1.6	2.9	6.6	3.8	5.2	3.0	3.8	2.6	2.7	12.2	1.4
	III ZCP1B3	3.2	11.5	11.0	4.8	5.8	6.7	4.1	4.1	4.2	4.3	6.5
	-- ZCP1C3	15.9	44.0	18.8	28.0	27.0	18.9	21.5	14.4	11.6	12.2	19.5
	III/III ZCP2D4	12.7	18.5	14.6	36.9	18.4	26.1	11.1	10.2	16.9	28.4	21.6
	III ZCP2G5-2	2.0	2.1	2.5	3.3	2.6	4.3	0.5	1.5	0.1	6.0	1.0
	I ZCP2G6-1	15.5	7.8	19.9	24.9	33.5	79.3	9.8	13.5	13.2	11.8	12.7
	I ZCP3B4	4.9	8.6	26.2	11.4	8.1	12.4	4.6	4.6	7.1	5.4	7.0
G2	I ZCP4C9	20.8	21.4	14.8	39.9	24.2	49.8	16.6	7.0	250.3	4.1	4.3
	I ZCP4D5-1	5.7	18.6	13.3	14.3	8.3	6.7	9.2	6.5	12.3	7.5	7.0
	I ZCP1B5-2	23.6	58.1	18.4	91.1	31.3	55.6	23.2	20.2	14.1	33.3	98.1
	III ZCP1B7-1	17.6	30.1	5.6	20.1	6.8	16.6	5.7	4.5	6.8	36.9	5.1
	-- ZCP1F7	5.9	20.1	15.4	13.6	9.4	9.2	9.4	9.7	4.2	18.3	8.3
	III/III ZCP2B10	25.9	104.5	64.4	161.8	46.4	84.0	45.7	45.4	23.8	31.2	86.5
G3	I ZCP2C11-2	17.8	37.4	16.9	89.7	21.6	59.8	34.1	59.6	38.7	25.8	28.2
	III ZCP2G11	1.6	8.8	6.0	6.4	2.5	9.2	7.8	9.3	13.7	8.7	4.0
	-- ZCP2C2	839.9	>2000	>2000	>2000	>2000	>2000	>2000	>2000	>2000	>2000	>2000
	-- ZCP2D5	811.0	>2000	>2000	>2000	601.9	637.2	125.8	230.4	>2000	>1000	930.3
	-- ZCP2E4	347.9	>2000	>2000	>2000	>2000	>2000	257.5	>2000	>2000	>2000	>2000
III ZCP4C2	693.8	987.4	704.8	>2000	>1000	1070	>2000	>2000	>2000	947.5	>2000	

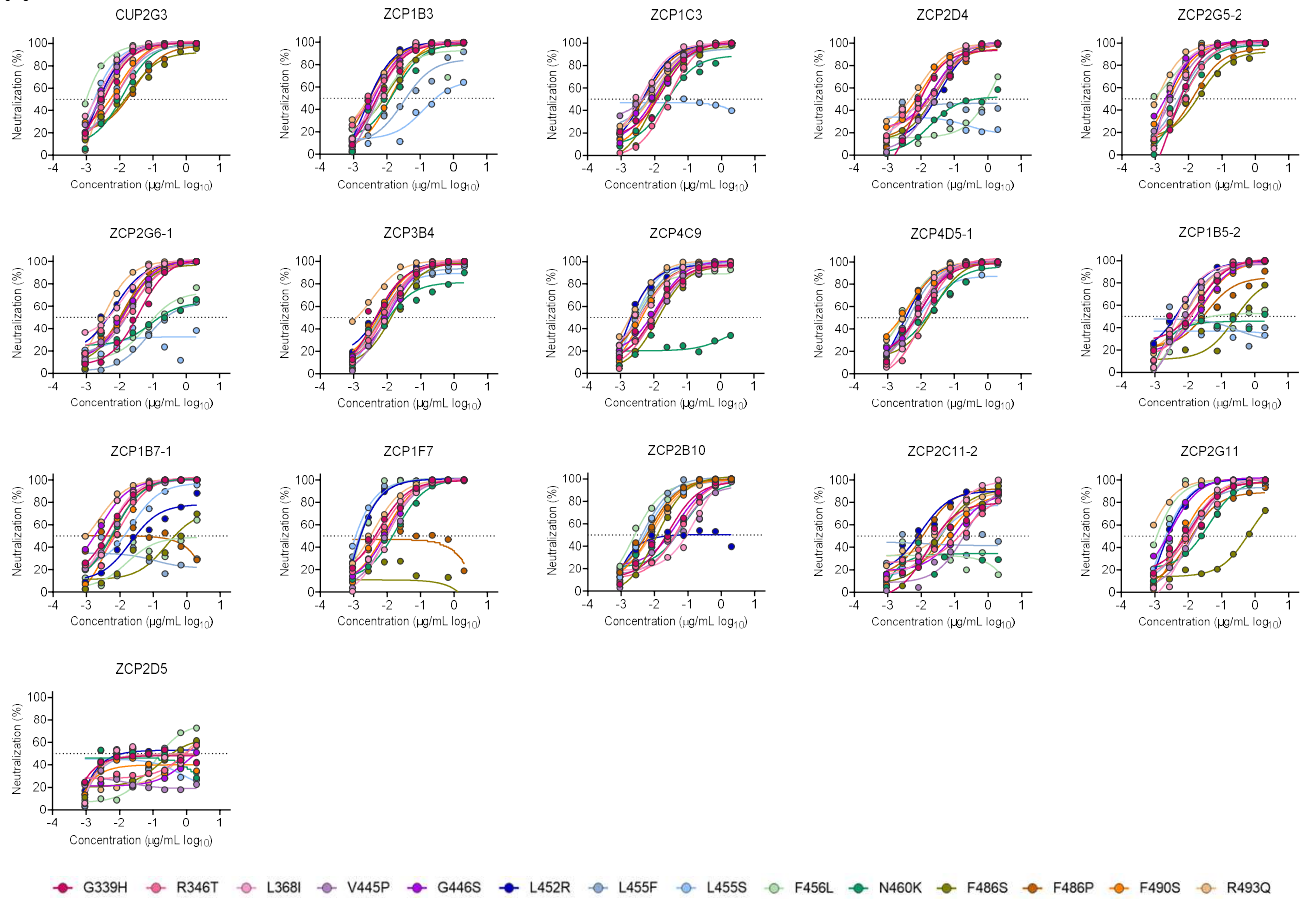
Figure S9. Diverse neutralization activity of RBD-specific NABs against Omicron BA.1 pseudoviruses with reversed mutations.

(A) Quantitative neutralization measurement of 19 anti-BA.1 NABs related to individual reversed mutations. The dashed line in each graph indicates 50% neutralization.

(B) Summary of IC₅₀ values. Ranges are indicated according to the color bar. The top three ultrapotent bnAbs are highlighted in red.

Figure S10

A



B

IC ₅₀ (ng/mL)		Relative to BA.2													
Class	Antibody	BA.2-D339H	BA.2-R346T	BA.2-L368I	BA.2-V445P	BA.2-G446S	BA.2-L452R	BA.2-L455F	BA.2-L455S	BA.2-F456L	BA.2-N460K	BA.2-F486S	BA.2-F486P	BA.2-F490S	BA.2-R493Q
G1	I CUP2G3	3.2	9.1	2.1	2.7	1.6	1.2	9.0	1.0	0.2	12.7	20.1	26.6	9.1	1.5
	III ZCP1B3	4.2	5.1	6.2	4.2	3.3	2.0	31.7	126.0	8.0	17.0	12.2	3.0	13.7	3.9
	-- ZCP1C3	18.0	26.1	4.2	12.8	11.9	4.6	11.7	>2000	10.0	22.9	9.2	6.4	11.0	11.3
	III/III ZCP2D4	5.5	34.0	12.3	24.0	28.8	37.4	>2000	>2000	1949	>1000	28.8	19.1	10.1	9.4
	III ZCP2G5-2	3.0	8.1	0.7	3.2	2.3	1.1	5.5	0.9	3.2	5.5	21.1	14.1	2.6	0.8
	I ZCP2G6-1	39.1	26.7	12.4	22.7	15.9	6.9	65.6	>2000	65.5	84.7	12.2	13.2	16.3	2.8
	I ZCP3B4	4.2	8.8	9.1	8.9	12.5	6.9	6.8	4.0	4.6	8.2	14.8	7.7	6.4	3.6
	I ZCP4C9	10.8	9.6	5.4	14.3	12.6	1.0	3.8	1.8	1.3	>2000	13.5	4.4	3.7	0.2
I ZCP4D5-1	9.6	11.6	5.8	7.1	10.8	2.9	4.1	8.0	3.3	22.3	23.1	7.1	4.3	3.5	
G2	I ZCP1B5-2	22.5	16.7	3.3	5.5	25.2	6.2	>2000	>2000	>1000	>1000	251.4	34.0	28.5	10.5
	III ZCP1B7-1	5.0	10.4	3.9	6.5	2.5	20.4	>2000	21.9	>1000	6.8	243.4	>2000	5.0	2.3
	-- ZCP1F7	5.9	8.1	9.1	10.1	10.2	0.6	0.7	0.4	0.4	18.9	>2000	>2000	8.5	3.9
	III/III ZCP2B10	28.4	51.7	174.2	55.6	48.2	>2000	4.5	4.9	2.2	74.1	11.8	7.5	8.0	10.2
	I ZCP2C11-2	15.0	202.7	44.7	208.0	111.2	9.5	>2000	26.4	>2000	>2000	36.9	12.8	68.1	66.3
	III ZCP2G11	12.7	12.7	8.6	14.9	3.0	1.4	7.6	1.2	0.5	42.0	686.0	10.8	5.5	0.5
G3	-- ZCP2D5	>2000	884.2	>2000	>2000	>1000	>1000	>2000	>2000	102.5	>2000	169.3	>1000	>2000	724.1

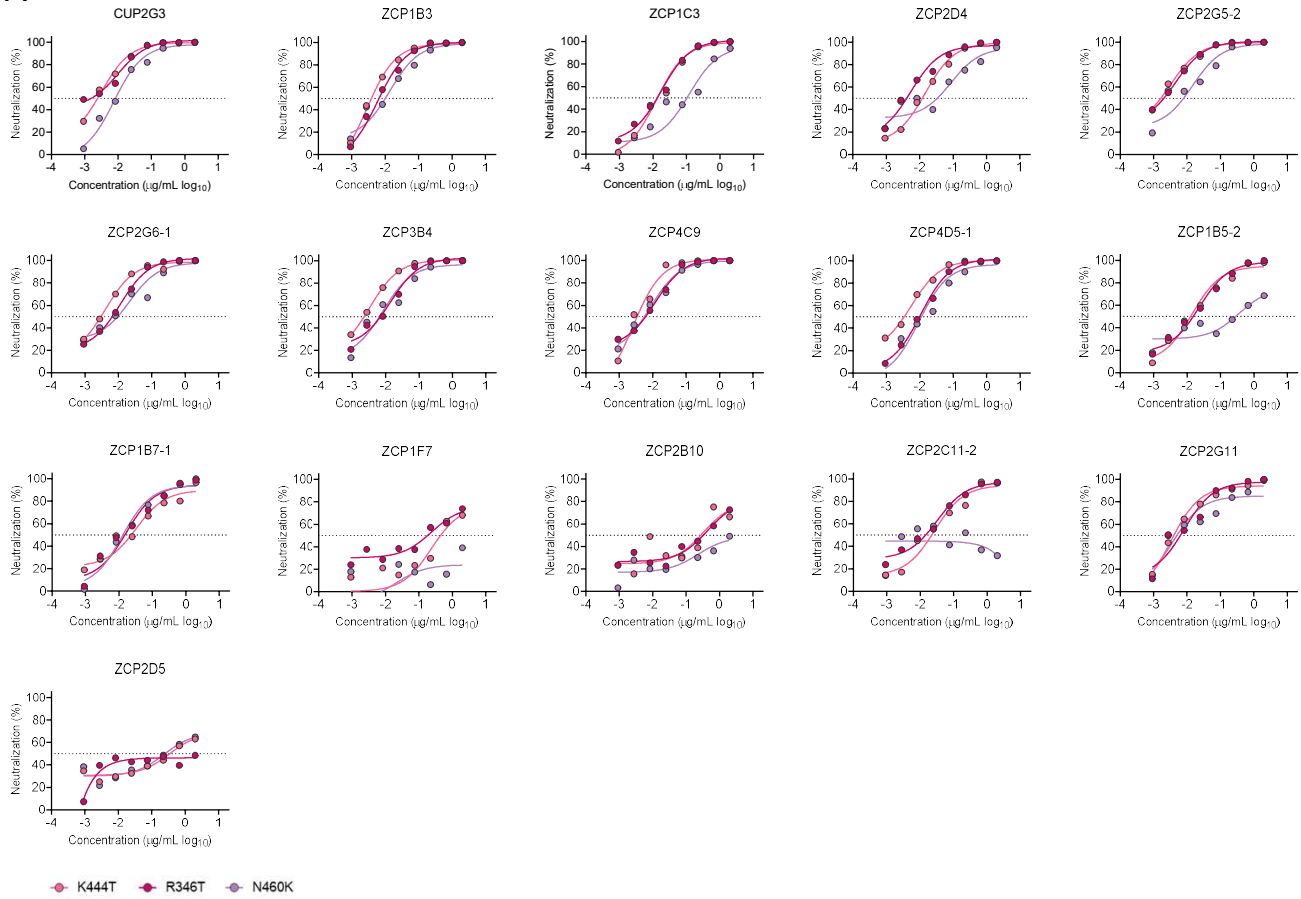
Figure S10. Diverse neutralization activity of RBD-specific NABs against Omicron BA.2 pseudoviruses with convergent mutations.

(A) Quantitative neutralization measurement of 16 anti-BA.2 NABs related to individual mutations. The dashed line in each graph indicates 50% neutralization,

(B) Summary of IC₅₀ values. Ranges are indicated according to the color bar. The top three ultrapotent bnAbs are highlighted in red.

Figure S11

A



B

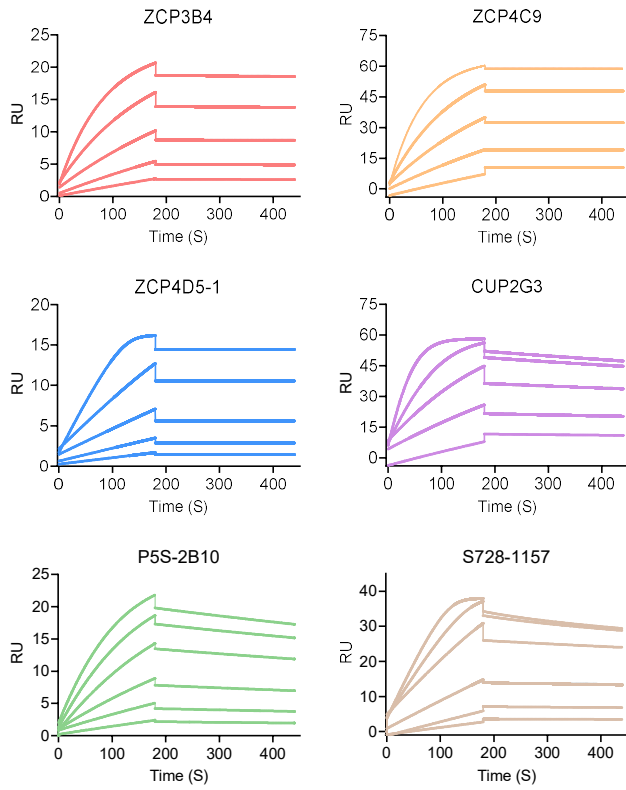
Class	Antibody	IC ₅₀ (ng/mL)		
		BA.4/5-R346T	BA.4/5-K444T	BA.4/5-N460K
G1	I CUP2G3	9.9	3.1	7.5
	VII ZCP1B3	5.9	2.8	13.6
	-- ZCP1C3	17.5	12.8	119.3
	VII/III ZCP2D4	5.4	14.6	85.9
	VII ZCP2G5-2	4.5	3.2	12.6
	I ZCP2G6-1	11.4	4.1	21.7
	I ZCP3B4	13.8	3.3	8.3
	I ZCP4C9	11.9	2.5	8.6
	I ZCP4D5-1	10.6	5.6	9.4
G2	I ZCP1B5-2	23.1	13.8	360.2
	VII ZCP1B7-1	16.5	32.9	12.4
	-- ZCP1F7	235.5	236.3	>2000
	VII/III ZCP2B10	439.4	323.9	>2000
	I ZCP2C11-2	32.0	27.1	>2000
	VII ZCP2G11	8.2	3.2	3.8
G3	-- ZCP2D5	>2000	343.3	233.1

Figure S11. Diverse neutralization activity of RBD-specific NAbs against Omicron BA.4/5 pseudoviruses with convergent mutations.

(A) Quantitative neutralization measurement of 16 anti-BA.4/5 NAbs related to individual mutations. The dashed line in each graph indicates 50% neutralization,

(B) Summary of IC₅₀ values. Ranges are indicated according to the color bar. The top three ultrapotent bnAbs are highlighted in red.

Figure S12



Antibody	BA.5 spike trimer		
	k_a ($M^{-1}s^{-1}$)	k_d (s^{-1})	K_D (nM)
ZCP3B4	2.23E+4	3.77E-5	1.69E-9
ZCP4C9	3.21E+4	4.45E-7	1.39E-11
ZCP4D5-1	1.52E+4	7.25E-7	4.77E-11
CUP2G3	8.48E+4	3.93E-4	4.64E-9
P5S-1H1	Undetectable	Undetectable	Undetectable
P5S-2B10	1.53E+5	5.80E-4	3.79E-9
S728-1157	1.04E+6	9.89E-4	9.53E-10

Figure S12. Binding kinetics of bNAbs ZCP3B4, ZCP4C9, ZCP4D5-1, CUP2G3, as well as control NAbs P5S-2B10 and S728-1157 to Omicron BA.5 spike trimer determined by surface plasmon resonance (SPR).

Figure S13

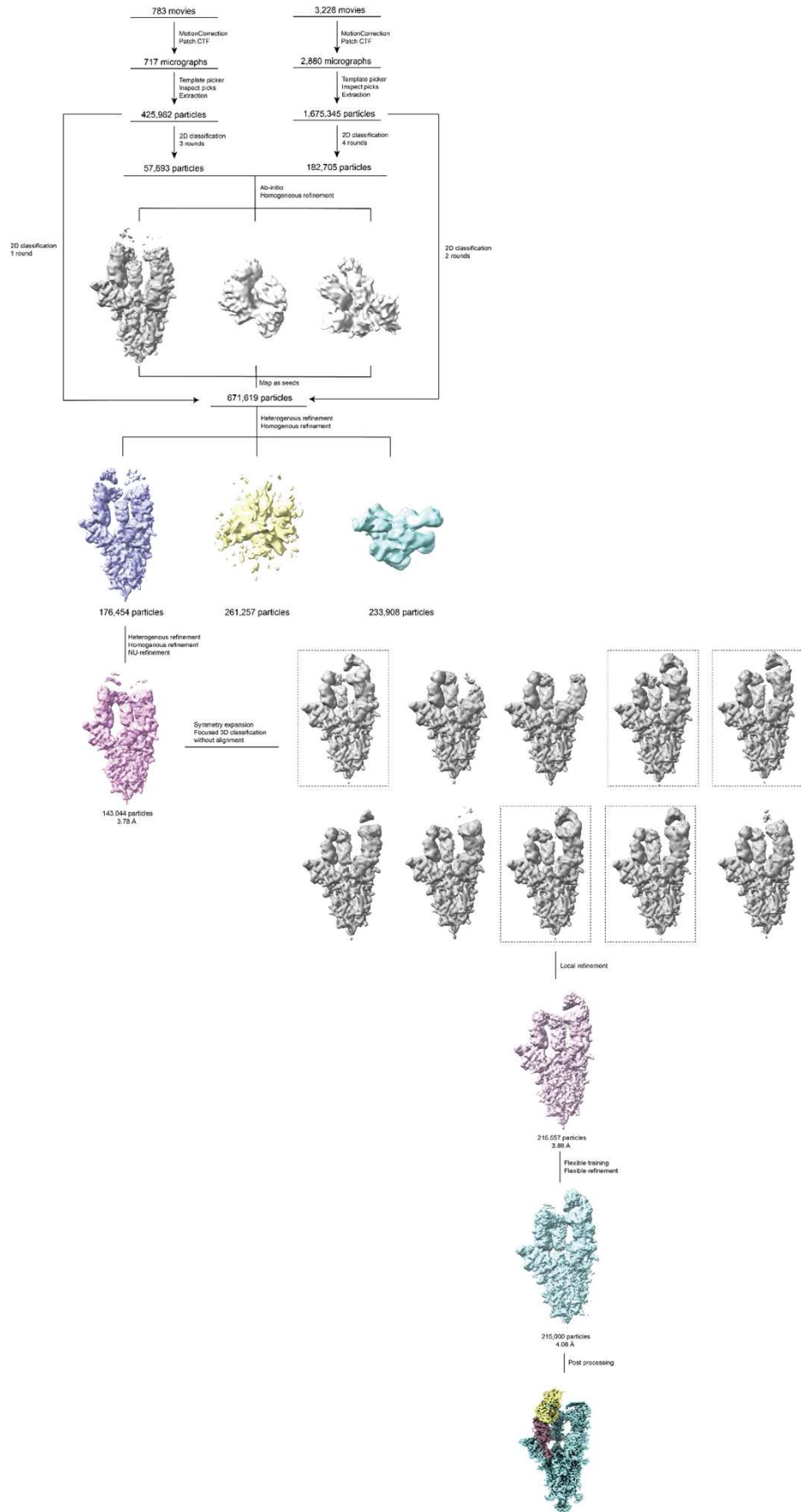


Figure S13. Cryo-EM data processing workflow of ZCP3B4 Fab-Omicron BA.5 spike complex.

Figure S14

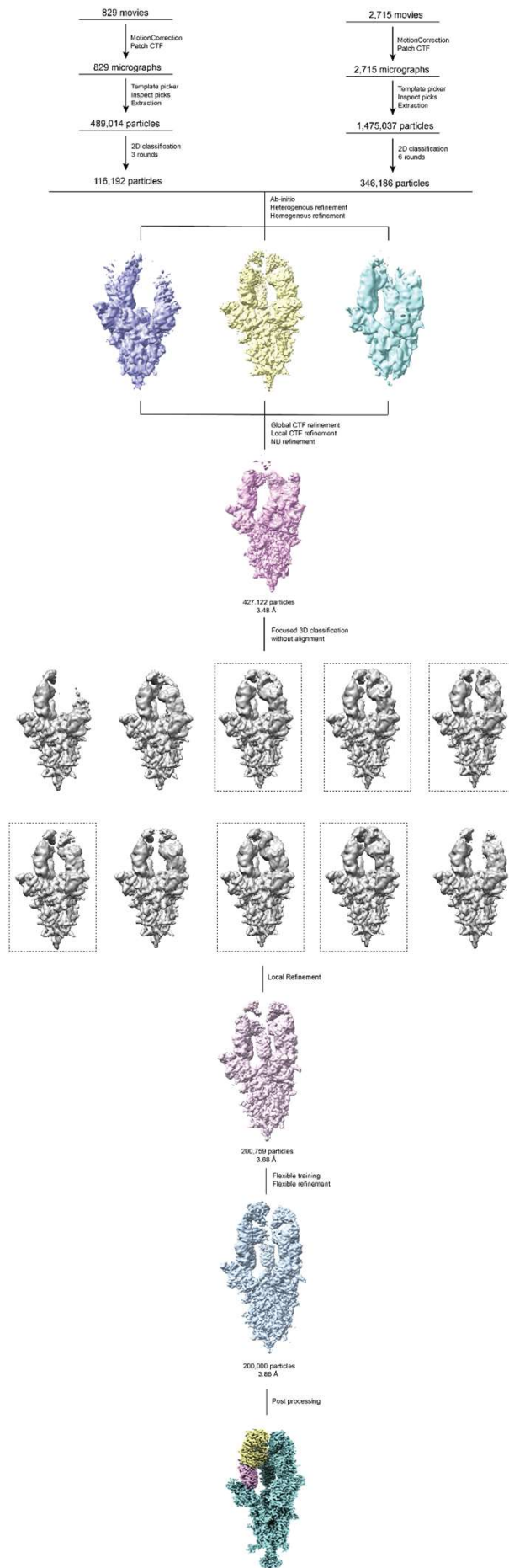


Figure S14. Cryo-EM data processing workflow of ZCP4C9 Fab-Omicron BA.5 spike complex.

Figure S15

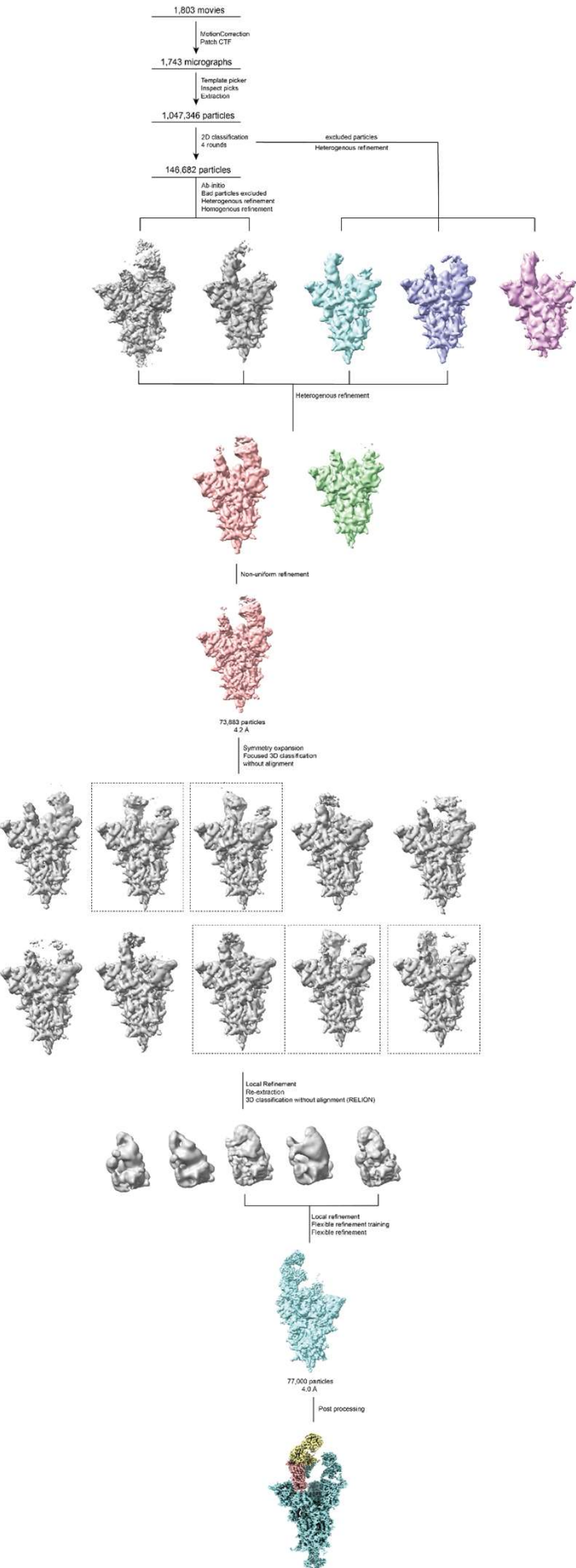


Figure S15. Cryo-EM data processing workflow of ZCP4D5-1 Fab-Omicron BA.5 spike complex.

Figure S16

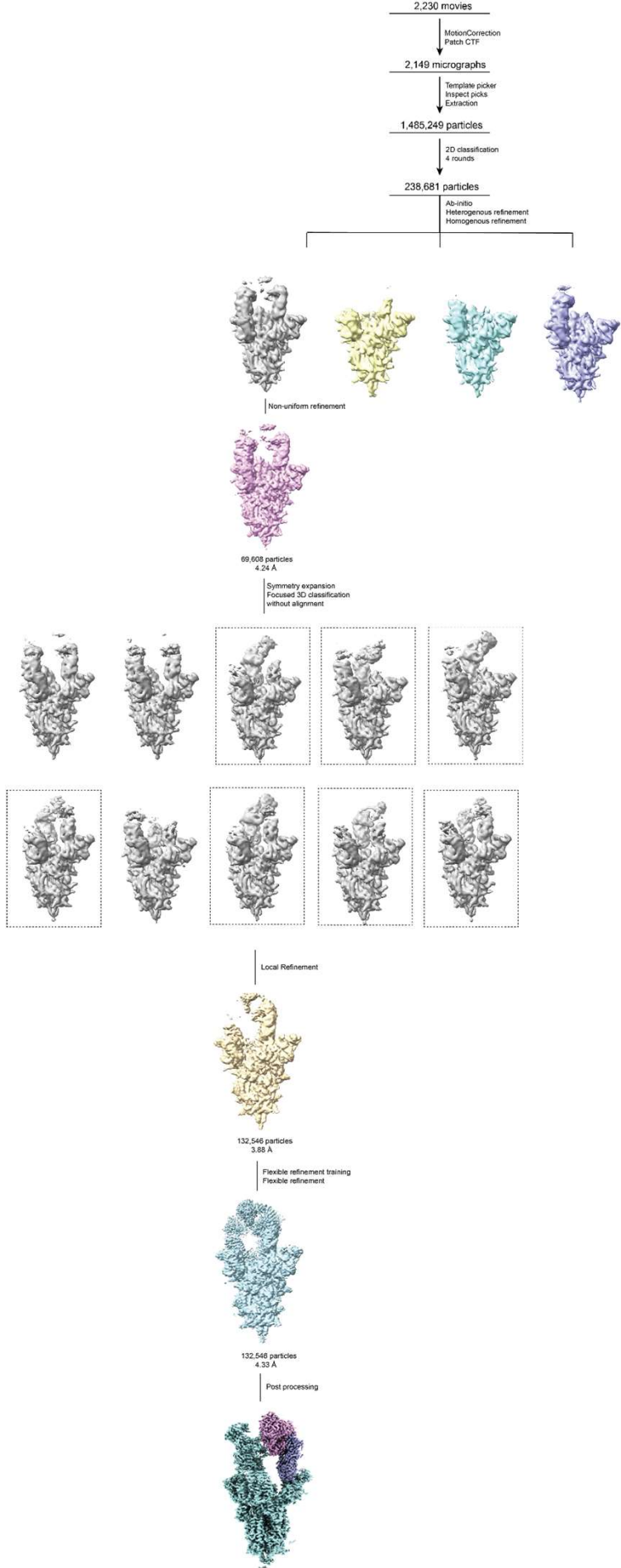


Figure S16. Cryo-EM data processing workflow of CUP2G3 Fab-Omicron BA.5 spike complex.

Figure S17

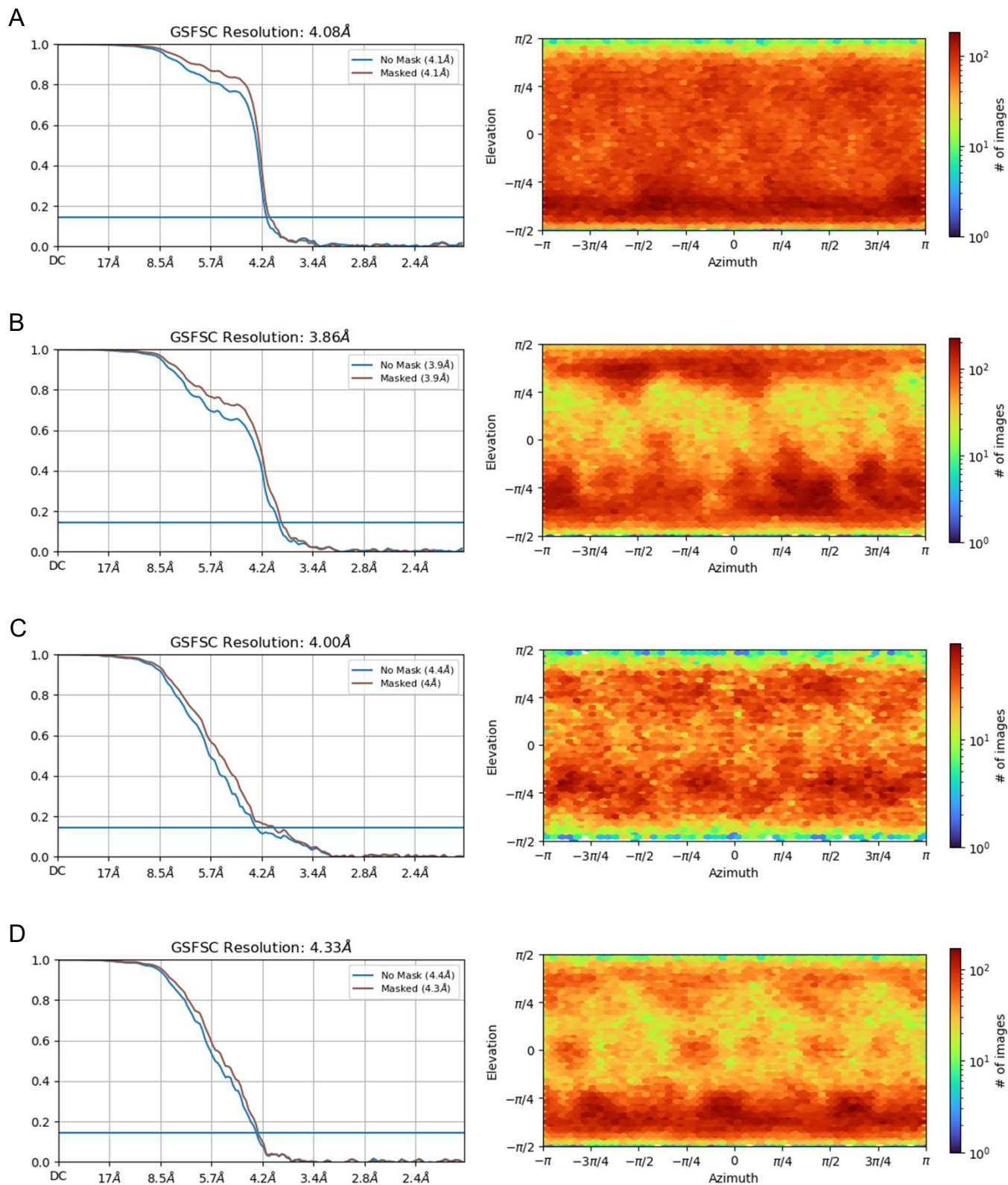
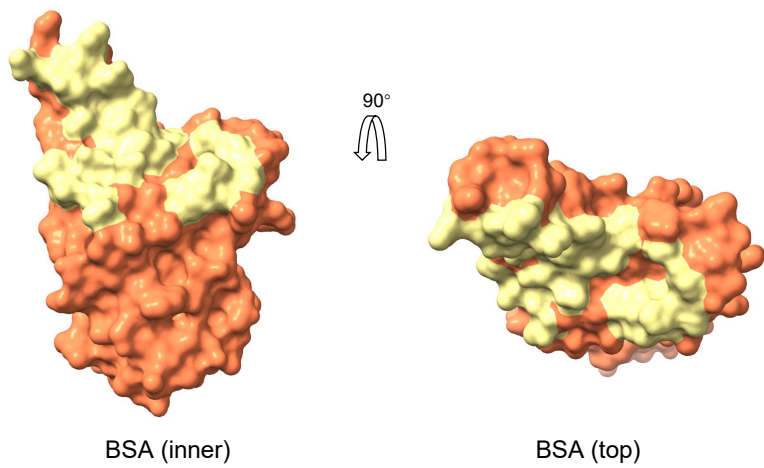


Figure S17. FSC curves and particle angular distribution display for map (A) ZCP3B4, (B) ZCP4C9, (C) ZCP4D5-1 and (D) CUP2G3.

A



B

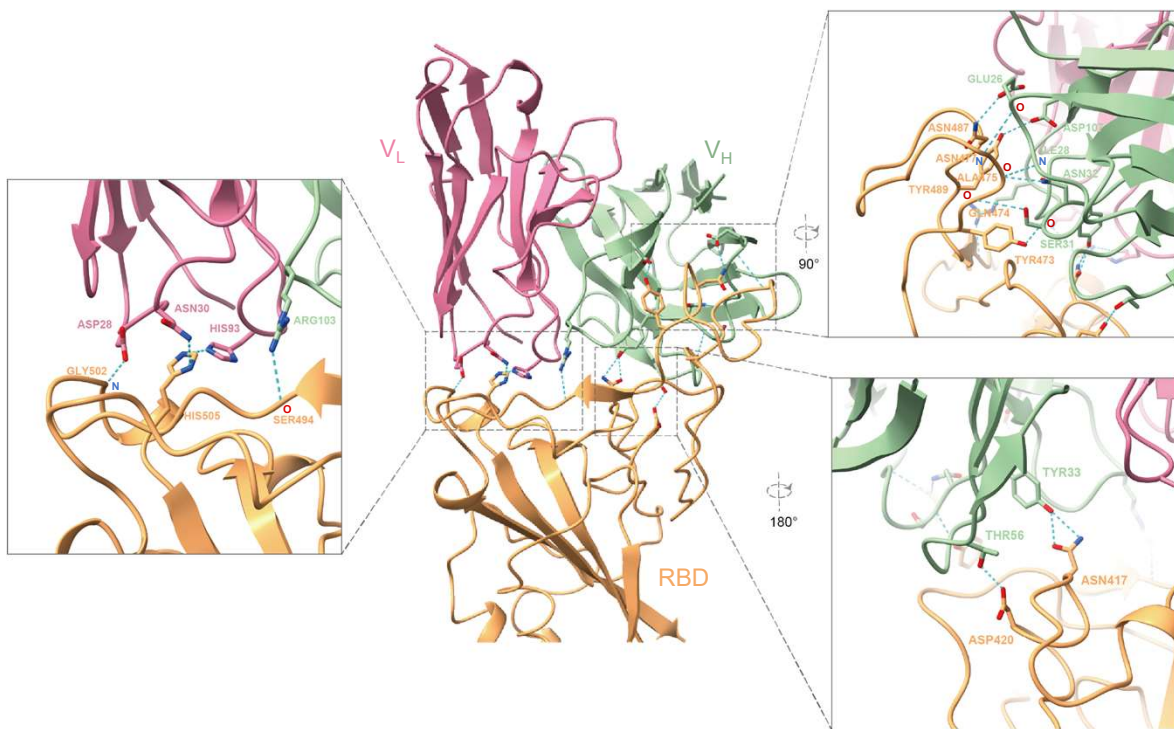
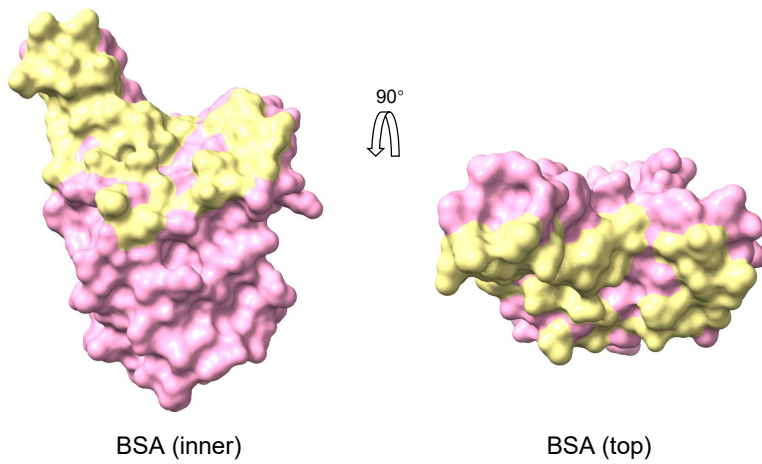


Figure S18. Interaction between bnAb ZCP3B4 Fab and Omicron BA.5 RBD.

(A) Buried surface area (BSA, yellow) of ZCP3B4 viewed from the RBD inner and top faces.

(B) Cartoon of ZCP3B4 variable regions binding RBD. The variable region of heavy chain (V_H), of light chain (V_L) and RBD are colored olive, pink and orange, respectively. The interface is zoomed in, and residues involved in the interaction are indicated. Hydrogen bonds are represented by blue dashed lines. Main chain carboxyl oxygen (O) or amine nitrogen (N) of antibodies and RBD for hydrogen bonds are shown.

A



B

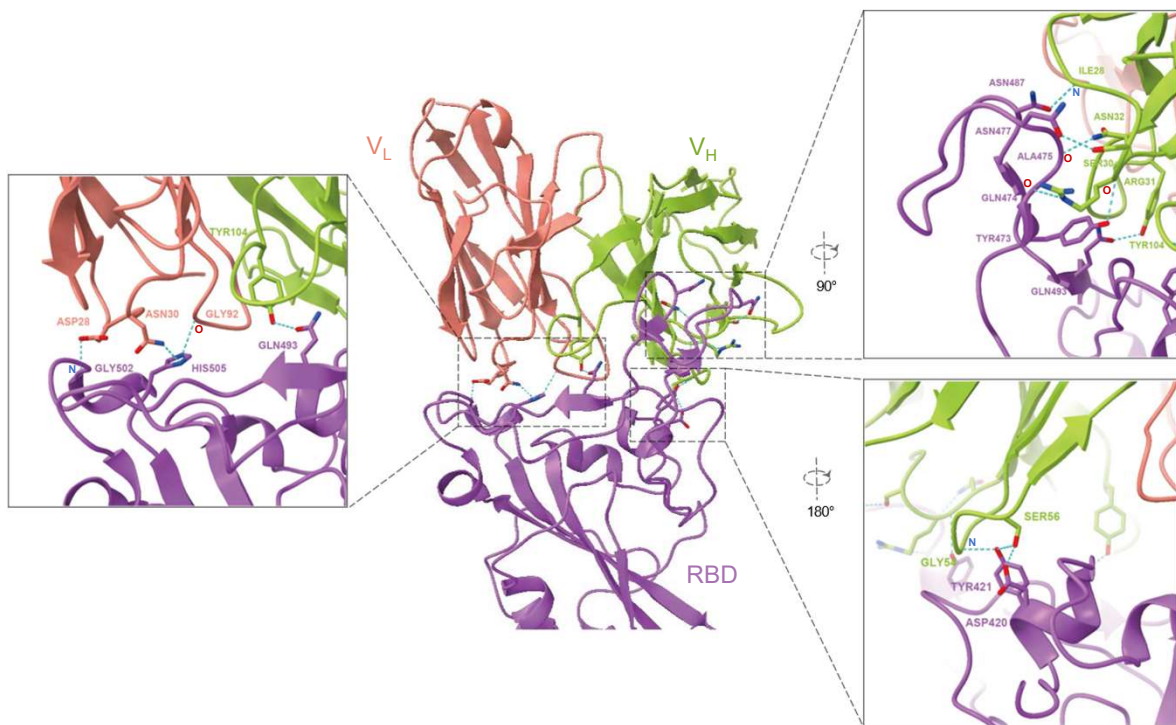


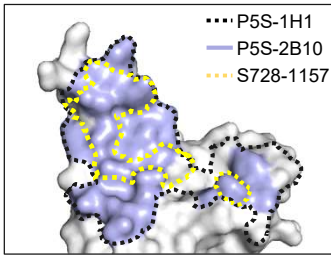
Figure S19. Interaction between bnAb ZCP4C9 Fab and Omicron BA.5 RBD.

(A) Buried surface area (BSA, yellow) of ZCP4C9 viewed from the RBD inner and top faces.

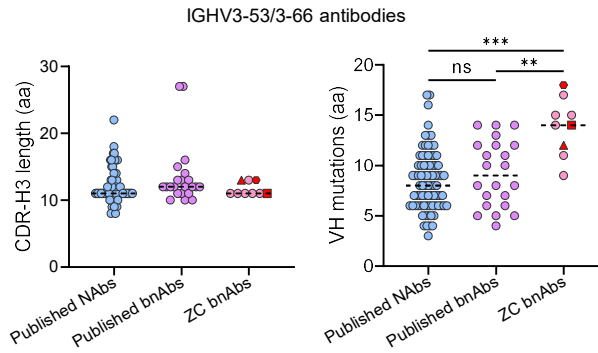
(B) Cartoon of ZCP4C9 variable regions binding RBD. The variable region of heavy chain (V_H), of light chain (V_L) and RBD are colored light green, light orange and purple, respectively. The interface is zoomed in, and residues involved in the interaction are indicated. Hydrogen bonds are represented by blue dashed lines. Main chain carboxyl oxygen (O) or amine nitrogen (N) of antibodies and RBD for hydrogen bonds are shown.

Figure S20

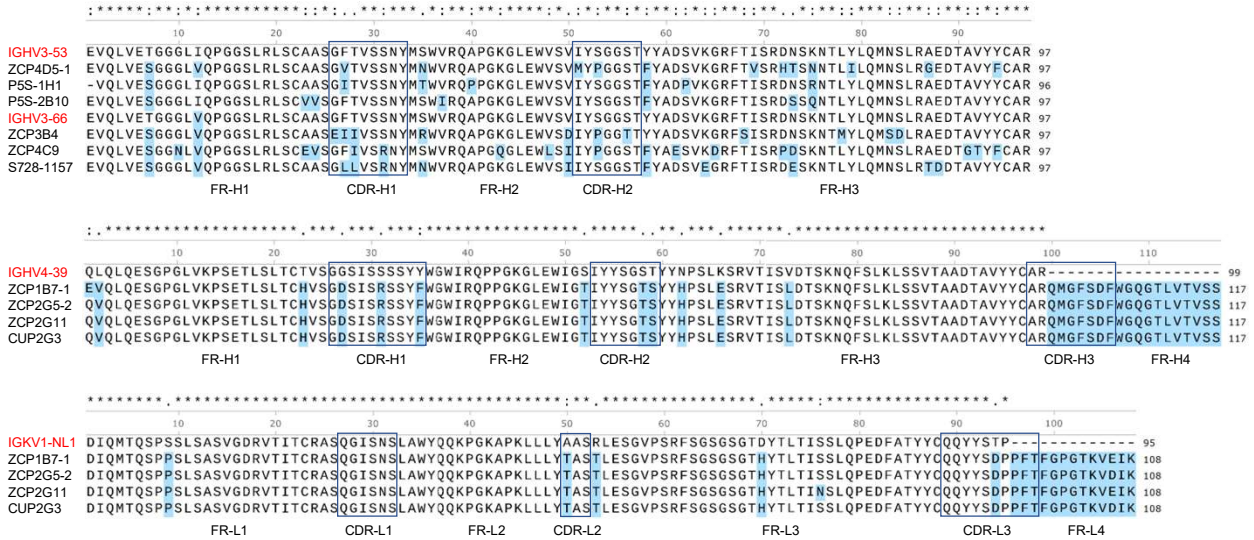
A



B



C



D

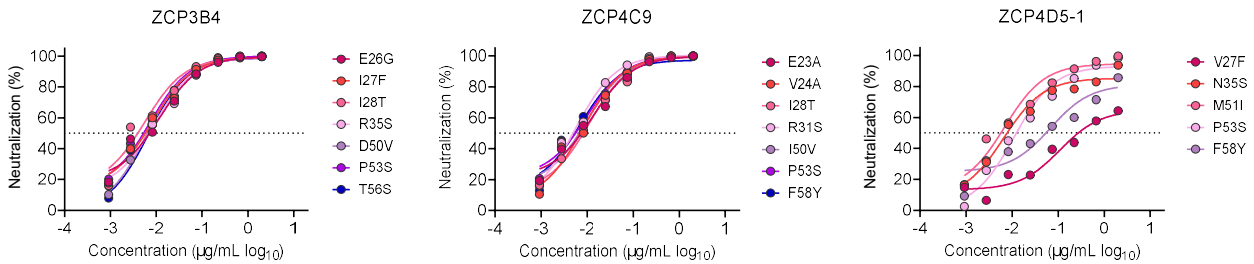


Figure S20. Molecular and genetic basis for neutralizing activity of bnAbs.

(A) Footprints of representative class I NAbS P5S-1H1 (black dotted line), P5S-2B10 (light purple) and S728-1157 (yellow dotted line) are shown on the surface of the BA.5 RBD.

(B) CDR3 lengths and mutation levels of IGHV3-53/3-66 NAb heavy chains. NAbS (anti-BA.1, n = 81) and bnAbS (anti-BA.1 and XBB, n = 22) reported in CoV-AbDab, as well as newly identified NAbS (n = 9) are shown. The triangle, hexagon and square represent ZCP3B4, ZCP4C9, and ZCP4D5-1, respectively. Comparisons were made by Kruskal-Wallis test followed by Dunn's multiple comparisons test. **p < 0.01, ***p < 0.001; ns (not significant), p > 0.05. aa, amino acid.

(C) Amino acid sequence alignments for VH of IGHV3-53/3-66 NAbS as well as for VH/VL of IGHV4-39/IGKV1-NL1 NAbS. Germline reference sequences are highlighted in red. CDR borders and numbering are shown according to the IMGT scheme.

(D) Neutralizing activity of bnAbS ZCP3B4, ZCP4C9 and ZCP4D5-1 with single germline-reverted substitutions in heavy chain against XBB.1.5. The dashed line in each graph indicates 50% neutralization.

Figure S21

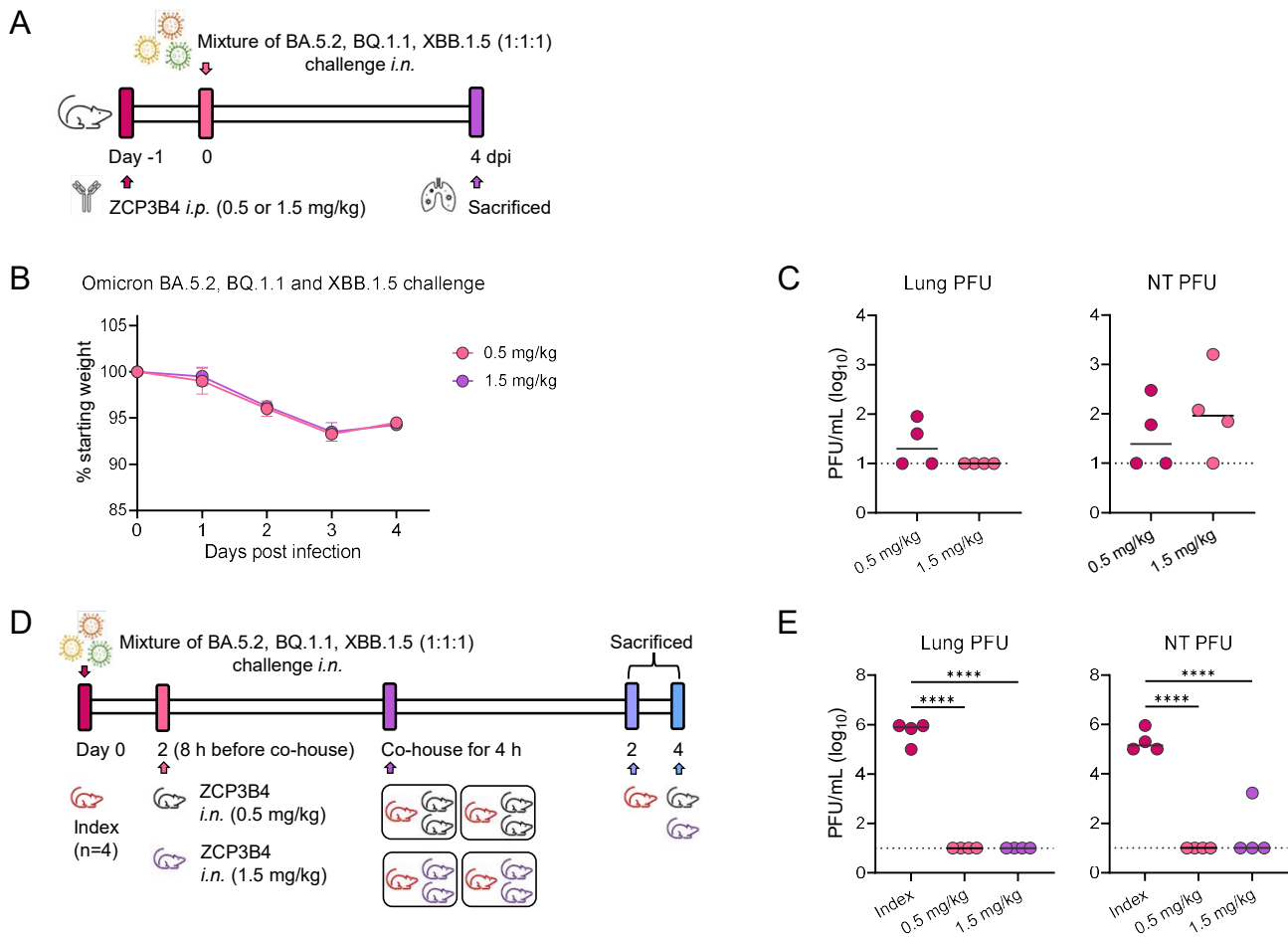


Figure S21. Efficacy of ZCP3B4 given at lower doses in preventing authentic Omicron BA.5.2, BQ.1.1 and XBB.1.5 infection in golden Syrian hamsters.

(A) Experimental schedule and color coding for the prophylaxis studies. Two groups of male hamsters received a single intraperitoneal injection of ZCP3B4 (0.5 mg/kg, n = 4; 1.5 mg/kg, n = 4) one day before viral infection (-1 dpi). 24 h later (day 0), each group was challenged intranasally with a mixture of live Omicron BA.5.2, BQ.1.1 and XBB.1.5 (10^5 PFU/hamster). All animals were sacrificed on day 4 for final analysis.

(B) Daily body weight change of each group was measured after direct infection. The data is shown as mean \pm SEM.

(C) Live viral plaque assay was used to quantify the number of infectious viruses in lungs and nasal turbinate (NT) homogenates of each group in the prophylaxis studies. Log₁₀-transformed plaque-forming unit (PFU) per mL was shown for each group. The dash line indicates the limit of detection. Each symbol represents an individual hamster with a line indicating the mean of each group.

(D) Experimental schedule and color coding for the contact transmission studies. Index hamsters (male, n = 4) were challenged intranasally with a mixture of live Omicron BA.5.2, BQ.1.1 and XBB.1.5 (10^5 PFU/hamster) two days prior to the co-housing (day 0). On 2 dpi, two groups of male hamsters were administered intranasally 0.5 or 1.5 mg/kg of ZCP3B4 (n = 4) 8 h before being co-housed with index hamsters at a 2:1 ratio. 4 h after the co-housing, index hamsters were sacrificed, whereas ZCP3B4-treated hamsters were separated and sacrificed on day 4 for final analysis.

(E) Live viral plaque assay was used to quantify the number of infectious viruses in lungs and NT of each group in the contact transmission studies. Log₁₀-transformed PFU per mL were shown for each group. The dash line indicates the limit of detection. Each symbol represents an individual hamster with a line indicating the mean of each group. Statistics were generated using one-way ANOVA followed by Tukey's multiple comparisons test. ****p < 0.0001.

Table S1

Donor ID	Age	Gender	Vaccination doses	Vaccine type	Days between the 1 st and 2 nd dose	Days between the 2 nd and 3 rd dose	Days between the 3 rd dose and symptom on set	Days between symptom on set and sample collection
CU-C3V-003	51	Male	3	Sinovac				
CU-C3V-028	41	Female	3	BNT162b2				
CU-C3V-033	49	Female	3	Sinovac				
CU-C3V-034	59	Male	3	Sinovac				
CU-C3V-041	44	Male	3	BNT162b2				
CU-C3V-044	49	Male	3	Sinovac				
CU-C3V-051	41	Male	3	BNT162b2	26 (21-36)	243 (189-274)	76 (45-104)	142 (130-148)
CU-C3V-052	37	Male	3	BNT162b2				
CU-C3V-058	41	Male	3	BNT162b2				
CU-C3V-059	51	Female	3	Sinovac				
CU-C3V-087	50	Female	3	BNT162b2				
ZC	59	Male	3	BNT162b2				

Table S1. Overview of the participants' samples included in this study.

Table S2

Area under curve (AUC)		Biotinylated target (class I-IV)				
		S2E12 (I)	LY-CoV555 (II)	LY-1404 (III)	S2X259(IV)	
Competitor	Control	4469.0	843.3	1837.0	204.8	
	G1					
		CUP2G3	1257.0	71.9	1438.0	144.3
		ZCP1B3	2039.0	365.3	1282.0	144.6
		ZCP1C3	3194.0	634.8	1306.0	251.9
		ZCP2D4	2016.0	459.1	1108.0	291.4
		ZCP2G5-2	951.4	276.6	2081.0	301.3
		ZCP2G6-2	2917.0	624.7	1978.0	317.0
		ZCP3B4	4207.0	389.0	1475.0	193.8
		ZCP4C9	4453.0	458.4	2050.0	167.1
		ZCP4D5-1	2913.0	208.4	1831.0	180.2
		G2				
		ZCP1B5-2	2840.0	632.2	2538.0	157.8
		ZCP1B7-1	1091.0	235.9	1226.0	218.4
		ZCP1F7	4655.0	642.2	1803.0	210.7
		ZCP2B10	3111.0	245.0	605.7	273.6
		ZCP2C11-2	2596.0	641.9	1356.0	285.3
		ZCP2G11	3120.0	75.5	1846.0	191.2
		G3				
		CUP3C9	4077.0	507.5	889.6	247.9
	ZCP2C2	4991.0	834.1	2051.0	238.2	
	ZCP2D5	4426.0	902.2	1936.0	251.9	
	ZCP2E4	4162.0	1512.0	671.9	1095.0	
	ZCP4C2	5442.0	807.4	986.3	233.4	

Table S2. Competition ELISA results of 20 RBD-specific NAbs in blocking binding of biotinylated class I-IV NAbs to the WT (D614G) spike trimer.

Shown is the area under curve (AUC) of targets in the presence of competitor-free control or competitors. The top three ultrapotent bnAbs are highlighted in red.

Table S3

	Antibody	IGHV gene	IGHD gene	IGHJ gene	CDR-H3	CDR-H3 length	Total identity
G1	CUP2G3	IGHV4-39	IGHD3-3	IGHJ4	ARQMGFSDF	9	92.3
	ZCP1B3	IGHV3-53	IGHD2-15	IGHJ6	ARDLVVFGMDV	11	92.5
	ZCP1C3	IGHV3-53	IGHD4-17	IGHJ4	ARGYGDYYFDY	11	90.8
	ZCP2D4	IGHV3-53	IGHD4-17	IGHJ4	ARAYGDYYFDY	11	95.2
	ZCP2G5-2	IGHV4-39	IGHD3-3	IGHJ4	ARQMGFSDF	9	92
	ZCP2G6-1	IGHV3-66	IGHD1-26	IGHJ6	VRPIMGARPGMDV	13	94.1
	ZCP3B4	IGHV3-66	IGHD1-26	IGHJ6	ARPIMGGRHGMDV	13	93.8
	ZCP4C9	IGHV3-66	IGHD3-3	IGHJ6	ARGLLEWRYGQDV	13	89.3
	ZCP4D5-1	IGHV3-53	IGHD4-17	IGHJ4	ARGYGDYYFDF	11	93.1
G2	ZCP1B5-2	IGHV3-53	IGHD2-15	IGHJ6	ARDLVVFGMDV	11	90.1
	ZCP1B7-1	IGHV4-39	IGHD3-3	IGHJ4	ARQMGFSDF	9	92.3
	ZCP1F7	IGHV1-58	IGHD2-2	IGHJ3	AAPYCNRTNCRDAFDS	16	91.7
	ZCP2B10	IGHV4-39	IGHD2-2	IGHJ6	VQVPVAMNGMDV	12	92.8
	ZCP2C11-2	IGHV3-53	IGHD5-12	IGHJ4	ARDRGRGDFDS	11	92.8
	ZCP2G11	IGHV4-39	IGHD3-3	IGHJ4	ARQMGFSDF	9	92.3
G3	CUP3C9	IGHV1-69	IGHD6-13	IGHJ4	ARRRLTPGIATTE	13	94.2
	ZCP2C2	IGHV1-18	IGHD2-2	IGHJ4	TRVEPRYCRSASCYTFEY	18	90.8
	ZCP2D5	IGHV4-39	IGHD2-2	IGHJ6	ARLGEHGYCSGTRCYDYFYGVVDV	23	95.0
	ZCP2E4	IGHV3-43	IGHD2-2	IGHJ6	AKDIDPCSSSSCYLTLFPNCGMDV	24	95.6
	ZCP4C2	IGHV3-23	IGHD2-2	IGHJ4	AKEEIFMPRLDFD	13	95.3
G4	ZCP1B10-1	IGHV1-69	IGHD3-10	IGHJ6	AKVDSPGMGRGIITFYHAMDV	21	94.2
	ZCP3C2-1	IGHV4-39	IGHD1-1	IGHJ6	VTATGDEYNPYHHGMEV	18	93.8

Table S3. Memory B cell-derived IGHV/D/J genes of 22 newly identified NAbs. The top three ultrapotent bnAbs are highlighted in red.

Table S4

	Antibody	IGKV gene	IGKJ gene	CDR-L3	CDR-L3 length	Total identity
G1	CUP2G3	IGKV1-NL1	IGKJ3	QQYYSDPPFT	10	96.8
	ZCP1B3	IGKV1-9	IGKJ3	QHLNSDLVT	9	96.8
	ZCP1C3	IGKV1-9	IGKJ3	QQVNS	5	97.1
	ZCP2D4	IGKV3-20	IGKJ2	QLSYT	5	96.7
	ZCP2G5-2	IGKV1-NL1	IGKJ3	QQYYSDPPFT	10	96.8
	ZCP2G6-1	IGKV1-33	IGKJ4	HQHDNLPLT	9	94.7
	ZCP3B4	IGKV1-33	IGKJ4	LQHDHVPLT	9	94
	ZCP4C9	IGKV1-33	IGKJ4	QQYGHQALS	9	93.9
	ZCP4D5-1	IGKV3-20	IGKJ2	QLSYT	5	95.6
G2	ZCP1B5-2	IGKV3-20	IGKJ5	QQYGSSPPIT	10	96.6
	ZCP1B7-1	IGKV1-NL1	IGKJ3	QQYYSDPPFT	10	96.8
	ZCP1F7	IGKV3-20	IGKJ1	QQYGNPWT	9	94.8
	ZCP2B10	IGKV2-28	IGKJ3	MQALQTPLIT	10	98.7
	ZCP2C11-2	IGKV1-33	IGKJ2	QQYDNLPSYT	10	95.8
	ZCP2G11	IGKV1-NL1	IGKJ3	QQYYSDPPFT	10	96.4
G3	CUP3C9	IGKV1-33	IGKJ2	QQYDNLPQT	9	97.6
	ZCP2C2	IGKV3-15	IGKJ1	QHYDNPPTWA	11	94.8
	ZCP2D5	IGKV3-15	IGKJ5	QQYNNWPPEIT	11	96.9
	ZCP2E4	IGKV3-20	IGKJ4	QLFDRSYG	8	95.1
	ZCP4C2	IGKV1-5	IGKJ1	QQYNSYSPTT	10	93.7
G4	ZCP1B10-1	IGKV3-20	IGKJ4	QQYGSSPLT	9	95.5
	ZCP3C2-1	IGKV3-11	IGKJ2	QQRSTWPRCT	10	98.6

Table S4. Memory B cell-derived IGKV/J genes of 22 newly identified NAbs. The top three ultrapotent bnAbs are highlighted in red.

Table S5

	ZCP3B4	ZCP4C9	ZCP4D5-1	CUP2G3
Data collection				
EM equipment	Titan Krios	Titan Krios	Titan Krios	Titan Krios
Voltage(kV)	300	300	300	300
Detector	Gatan K3 summit	Gatan K3 summit	Gatan K3 summit	Gatan K3 summit
Magnification	81,000x	81,000x	81,000x	81,000x
Electron dose (e/Å ²)	50	50	50	50
Defocus range (µm)	-1.0~-2.5	-1.0~-2.5	-1.0~-2.5	-1.0~-2.5
Pixel size (Å)	1.06	1.06	1.06	1.06
Collected movies	4,111	3,544	1,801	2,230
Reconstruction				
Software	cryoSPARC v 4.1.2, RELION 4.0			
Final particles	215,557	200,759	102,432	132,546
B-factors (Å ²)	-120.2	-99.4	-127.9	-111.3
Map resolution (Å)	3.88(0.143)	3.68(0.143)	4.18(0.143)	3.88(0.143)
Atomic modeling				
Software	UCSF Chimera, ChimeraX, Coot, Phenix		N/A	
Chain	3	3		
Residues	414	414		
Water	0	0		
Atoms	3224 (Hydrogens:0)	3246 (Hydrogens:0)		
RMSD Length (Å)	0.014	0.014		
RMSD Angles (Å)	1.836	1.853		
Ramachandran plot (%)				
Favored	94.58	92.86	N/A	
Allowed	4.68	7.14		
Outliers	0.74	0		
Rotamer outliers	0.57	0.85		
C-beta outliers	0.53	0		

Table S5. Statistics of cryo-EM data collection, processing and model refinement.

Table S6

Antibody	Buried surface area (BSA)	BSA residues in RBD
ZCP3B4	Heavy chain: 773.9 Å ² Light chain: 209.0 Å ²	T415, N417, D420, Y421, L455, F456, S459, N460, Y473, A475, G476, N477, V486, N487, Y489, Q493, S494
ZCP4C9	Heavy chain: 941.1 Å ² Light chain: 360.3 Å ²	N405, Q409, Q414, T415, N417, Y421, Y453, L455, F456, K458, S459, Y473, Q474, A475, G476, N477, K478, V486, N487, Y489, Q493, S494, G496, R498, T500, Y501, G502, G504, H505
ZCP4D5-1	Heavy chain: 728.9 Å ² Light chain: 383.8 Å ²	N417, D420, Y421, Y449, Y453, L455, F456, Y473, A475, N477, V486, N487, Y489, F490, Q493, S494, G496, R498, T500, Y501, G502, H505
CUP2G3	Heavy chain: 692.7 Å ² Light chain: 827.3 Å ²	R403, N405, Q409, T415, G416, N417, D420, Y421, G446, Y449, R452, Y453, L455, F456, R457, Y473, A475, G476, N477, A484, G485, V486, N487, Y489, Q493, S494, G496, R498, T500, Y501, G502, H505

Antibody	ZCP3B4	ZCP4C9
Epitopes	N417, D420, Y473, Q474, A475, N477, N487, Y489, Q493, S494, G502, H505	D420, Y421, Y473, Q474, A475, N477, N487, Q493, G502, H505

Table S6. Buried surface area (BSA) and epitopes of bnAbs in Omicron BA.5 RBD.

Residues with at least residue-area buried (default 15 Å²) are considered as BSA residues (top).

BA.5 mutation sites involved in epitopes (bottom) are highlighted in red.